
Data augmentation in Bayesian neural networks and the cold posterior effect

Seth Nabarro*

Department of Computing
Imperial College London
London, SW7 2BX, UK
seth.nabarro09@imperial.ac.uk

Stoil Ganev*

Department of Computer Science
University of Bristol
Bristol, BS8 1UB, UK

Adrià Garriga-Alonso

Department of Engineering
University of Cambridge
Cambridge, CB2 1PZ, UK
ag919@cam.ac.uk

Vincent Fortuin

Department of Computer Science,
ETH Zürich,
Zürich, Switzerland

Mark van der Wilk†

Department of Computing
Imperial College London
London, SW7 2BX, UK
m.vdwilk@imperial.ac.uk

Laurence Aitchison†

Department of Computer Science
University of Bristol
Bristol, BS8 1UB, UK
laurence.aitchison@gmail.com

Abstract

Data augmentation is a highly effective approach for improving performance in deep neural networks. The standard view is that it creates an enlarged dataset by adding synthetic data, which raises a problem when combining it with Bayesian inference: how much data are we really conditioning on? This question is particularly relevant to recent observations linking data augmentation to the cold posterior effect. We investigate various principled ways of finding a log-likelihood for augmented datasets. Our approach prescribes augmenting the same underlying image multiple times, both at test and train-time, and averaging either the logits or the predictive probabilities. Empirically, we observe the best performance with averaging probabilities. While there are interactions with the cold posterior effect, neither averaging logits or averaging probabilities eliminates it.

1 Introduction

Data augmentation (Shorten & Khoshgoftaar, 2019) is a fundamental technique for obtaining high performance in modern neural networks (NNs). In computer vision, data augmentation involves creating synthetic training examples by making small modifications, such as a rotation or crop, to the input image.

At the same time, Bayesian inference allows us to reason about uncertainty in neural network weights (MacKay, 1992; Welling & Teh, 2011; Blundell et al., 2015; Fortuin, 2021) given limited data. Bayesian inference is particularly important in safety-critical settings such as self-driving cars or medical imaging where it is crucial to be able to hand over to a human when uncertainty is too large.

* equal contribution

† equal contribution

However, in these settings we still need good performance, so we need to combine Bayesian inference and data augmentation. Bayesian uncertainty estimates depend fundamentally on the number of datapoints, with more uncertainty when less data is available. This raises a key problem when trying to combine Bayesian inference and data augmentation: how many data points do we really have—is it just the size of the underlying dataset, or does it include all the augmented images?

To address this question, it is important to consider the cold posterior effect, in which artificially reducing uncertainty by taking the posterior to a power greater than 1 dramatically improves performance (Wenzel et al., 2020). This has the same effect on the likelihood as increasing the number of training points. The cold posterior effect is puzzling: if the prior accurately expresses our uncertainty, then the Bayesian posterior should be optimal, and artificial changes such as a “cold” posterior should be detrimental to performance. To confuse matters further, several researchers recently found that the cold posterior effect disappears if we do not use data augmentation in some cases (Wenzel et al., 2020; Fortuin et al., 2021b; Izmailov et al., 2021), so there seem to be strong interactions between data augmentation and the cold posterior effect.

While the simplicity of data duplication is appealing, there is a fundamental issue: we often have infinitely many augmented images (e.g. if we consider a real-valued rotation). Using infinitely many datapoints in Bayesian inference usually results in ignoring the prior and shrinking uncertainty to zero. Such a posterior is not sensible in image classification where the number of training examples is ultimately limited.

As such, we need alternative approaches to combining Bayesian inference and data augmentation, and to understanding their interaction with the cold posterior effect. In particular, we consider incorporating data augmentation into the Bayesian generative model. The resulting models augment one underlying image multiple times and average either the logits or the probabilities output by the model, both at train and test-time. We find that this approach improves performance even in a non-Bayesian setting with fixed computational budget. While averaging logits or averaging probabilities both give a principled method to combine data augmentation and Bayesian inference, we find the cold posterior effect is still present with these approaches.

Our results have important implications for the cold posterior effect. In particular, both averaging logits and averaging probabilities can be seen as improvements to the prior over functions. The same can be said of recent work showing that, at least in large-scale convolutional networks, using a prior with spatial correlations in the weights improved performance but did not eliminate the cold posterior effect (Fortuin et al., 2021b). In combination, these results suggest that perhaps the cold posterior effect in large-scale convolutional networks does not emerge due to a misspecified prior (though there could always be better priors that have not yet been considered). This would support an alternative hypothesis, of a misspecified likelihood which fails to account for the effects of data curation in benchmark datasets such as CIFAR-10 (Aitchison, 2020) (see Sec. 6 for further details).

2 Contributions

1. We give a conditional independence argument to show that treating each augmented image as a separate datapoint is not viable (Sec. 3.2).
2. We implement two principled data augmentation likelihoods for neural networks (Sec. 4) based on:
 - averaging predictive probabilities (this appears in Appendix K of Wenzel et al. (2020), but they only gave a training objective for the trivial case of one augmentation sample; for which averaging probabilities and logits is equivalent to standard data augmentation).
 - averaging logits (investigated in kernel models, e.g. Van der Wilk et al., 2018; Dao et al., 2019).
3. We show that principled data augmentation priors with multiple training augmentations for each original unaugmented image may be beneficial even in non-Bayesian models using stochastic gradient descent (SGD) with a fixed computational cost (Sec. 5.1).
4. We compare the performance of averaging logits vs. averaging probabilities, and find that averaging probabilities performs marginally better (Sec. 5.1 and 5.2).
5. We show that the cold posterior effect persists when using principled data augmentation priors (Sec. 5.2).

3 Background

3.1 Data augmentation

In supervised learning problems, we are interested in learning some unknown functional relationship $f : \mathcal{X} \rightarrow \mathcal{Y}$ from example input-output pairs $(\mathbf{x}_i, y_i), i = 1, \dots, N$. Given a particular learning method, we can usually expect better performance when more examples are given (Loog et al., 2019). In many settings, we have information about *invariances* that exist in a certain problem, i.e. the knowledge that the function does not change its output for certain transformations of the input. The most basic form of data augmentation takes advantage of this information by applying the transformations to the inputs and copying the output value, to create additional input-output pairs, which are then included in training. Often, the amount of additional “augmented data” can be unbounded, for example when allowable transformations are specified in a continuous range, e.g. rotations. This simple procedure has been very successful in improving performance in a wide variety of machine learning methods (Loosli et al., 2007; Krizhevsky et al., 2012; Bishop, 2006). Recent work has analysed the effect of data augmentation on invariances in the functions that are learned (Dao et al., 2019; Chen et al., 2020).

3.2 Bayesian inference

Bayesian inference allows us to infer a distribution over our parameters of interest, concretely addressing the estimation of uncertainty. It prescribes a strict procedure for updating beliefs about unknown quantities in light of observed data. The model is specified by a prior on the weights $P(\mathbf{w})$ and a likelihood $P(\mathbf{y}|\mathbf{w}, \mathbf{X}) = \prod_{i=1}^N P(y_i|\mathbf{w}, \mathbf{x}_i)$. Thus, the log-posterior is given by

$$\log P(\mathbf{w}|\mathbf{X}, \mathbf{y}) = \log P(\mathbf{w}) + \sum_{i=1}^N \mathcal{L}^i(y_i; \mathbf{w}) + \text{const}. \quad (1)$$

Without augmentation, the multi-class classification log-likelihood is given by

$$\mathcal{L}_{\text{noaug}}^i(y_i; \mathbf{w}) = \log P_{\text{noaug}}(y_i|\mathbf{w}, \mathbf{x}_i) = \log \text{softmax}_{y_i} f(\mathbf{x}_i; \mathbf{w}), \quad (2)$$

where $f(\mathbf{x}_i; \mathbf{w})$ is a vector of logits output by the neural network.

In Bayesian inference, we are free to choose the prior and likelihood, but not the way they are combined to find the posterior. This presents a challenge for data augmentation when formulated as a change in the dataset size. Changing the dataset size through augmentation is inconsistent with the Bayesian principle of requiring the likelihood to be a valid probability distribution for the data conditioned on the parameters. Ignoring this fundamental issue, suppose we were to go ahead anyway, and include a likelihood term for all augmented versions of each input, $\mathbf{x}'_{i,a}$, we obtain

$$\mathcal{L}_{\text{add}}^i(y_i; \mathbf{w}) = \sum_{a=1}^A \log \text{softmax}_{y_i} f(\mathbf{x}'_{i,a}; \mathbf{w}). \quad (3)$$

Here A is the total number of augmentations, and a indexes different augmentations of the same underlying image. This is likely to result in a posterior which is overconfident, as it assumes A times more data points than we really have. The infinite augmentation case is particularly problematic, as it results in ignoring the prior, which is clearly unjustified given all our examples are generated from a finite set of underlying observations.

This issue is really hinting at a deeper problem: in treating each augmented input as a separate datapoint, we have implicitly assumed that the label for each augmentation of the same input is independent (conditioned on the input). This could be achieved if we took each augmentation of the same underlying input and presented them to a different human annotator. However, that is not what happens in practice. Usually only the underlying unaugmented input is labelled by a human, and the label is assumed to be the same for all resulting augmentations. As such, a mistaken label will propagate to all the augmented examples, and thus the labels for different augmentations of the same underlying input are not independent and an approach (such as this one), which assumes they are, cannot be valid.

By far the most common approach in past work combining data augmentation and Bayesian inference is to take a pre-existing algorithm, and replace the underlying non-augmented image, \mathbf{x}_i , with an

augmented image, \mathbf{x}'_i . Ultimately, this targets the averaged (negative) loss (Appendix A)

$$\mathcal{L}_{\text{loss}}^i(y_i; \mathbf{w}) = \mathbb{E}[\log \text{softmax}_{y_i} f(\mathbf{x}'_i; \mathbf{w})]. \quad (4)$$

This approach is convenient, since a single sample from the augmentation distribution can provide an unbiased estimate $\hat{\mathcal{L}}_{\text{loss}} = \log \text{softmax}_{y_i} f(\mathbf{x}'_i; \mathbf{w})$, so it is used explicitly in some settings (e.g. Benton et al., 2020). Importantly, though, a valid likelihood should arise from a valid distribution over labels, and should therefore normalise if we sum over labels. For instance, without augmentation, we have

$$1 = \sum_{y_i=1}^Y \exp \mathcal{L}_{\text{noaug}}^i(y_i; \mathbf{w}). \quad (5)$$

However, $\mathcal{L}_{\text{loss}}^i(y_i; \mathbf{w})$ does not in general normalise to 1 and thus it does not form a valid log-likelihood.

3.3 The cold posterior effect

The discussion above highlights that the number of datapoints, and hence the uncertainty, is unclear when using data augmentation in combination with Bayesian inference. Interestingly, we can often dramatically improve the performance of a Bayesian NN by artificially reducing uncertainty by taking the posterior to the power of $1/T$ where $0 < T < 1$,

$$Q(\mathbf{w}) \propto P(\mathbf{w}|\mathbf{X}, \mathbf{y})^{1/T} \propto P(\mathbf{w})^{1/T} \prod_{i=1}^N P(y_i|\mathbf{w}, \mathbf{x}_i)^{1/T}. \quad (6)$$

This is known as the cold posterior effect (Wenzel et al., 2020). Note that the cold posterior effect is typically seen when using $\mathcal{L}_{\text{loss}}$ to incorporate augmentation (Appendix A, Wenzel et al., 2020), so it might be analogous to artificially reducing uncertainty by treating each augmented image as a separate datapoint.

4 Methods

To obtain a principled log-likelihood incorporating data augmentation, we cannot take the standard approach of just using augmented data in a pre-existing algorithm. Instead, we need to build data augmentation into the probabilistic generative model describing the likelihood. To do this, we consider priors in which the output class label is given by averaging over a distribution of all possible augmentations of a single underlying image, while ensuring that normalization (Eq. 5) is satisfied. In doing so, we circumvent the need to find the “true” number of examples in our augmented dataset. There are two justifications for these averaging schemes. Firstly, averaging over an augmentation group creates an invariance, which is how data augmentation was first brought into the Bayesian framework in the context of GPs by Van der Wilk et al. (2018). Secondly, there is the graphical model introduced by Wenzel et al. (2020). Here, we discuss how both views lead to simple and highly similar methods.

In a classification setting, we have a choice as to which quantity we average, and hence at which level we enforce the invariance: at the level of logits or predictive probabilities, that is,

$$p_{\text{inv}}(\mathbf{x}; \mathbf{w}) = \int d\mathbf{x}' P(\mathbf{x}'|\mathbf{x}) \text{softmax} f(\mathbf{x}'; \mathbf{w}) = \mathbb{E}[\text{softmax} f(\mathbf{x}'; \mathbf{w})], \quad (7)$$

$$f_{\text{inv}}(\mathbf{x}; \mathbf{w}) = \int d\mathbf{x}' P(\mathbf{x}'|\mathbf{x}) f(\mathbf{x}'; \mathbf{w}) = \mathbb{E}[f(\mathbf{x}'; \mathbf{w})]. \quad (8)$$

Here $P(\mathbf{x}'|\mathbf{x})$ is the distribution over augmented images \mathbf{x}' given the original image \mathbf{x} , and $f(\mathbf{x}'; \mathbf{w})$ is the vector of logits output by the neural network for an augmented input. The quantity $f_{\text{inv}}(\mathbf{x}; \mathbf{w})$ is the invariant vector of logits given by averaging logit vectors for different augmentations of the same underlying image. $p_{\text{inv}}(\mathbf{x}; \mathbf{w})$ is the invariant vector of probabilities given by averaging the predicted probabilities over the augmentations. Here and subsequently, we take expectations over one, \mathbf{x}'_i , or multiple, $\mathbf{x}'_{i,k}$, augmentations, conditioned on the underlying image, \mathbf{x}_i . We derive the resulting lower bounds of the log-likelihoods for both cases here, and evaluate them empirically in Sec. 5.

The exact but intractable log-likelihood terms, for averaging logits and averaging probabilities are

$$\mathcal{L}_{\text{prob}}^i(y_i; \mathbf{w}) = \log P_{\text{prob}}(y_i | \mathbf{x}_i, \mathbf{w}) = \log \mathbb{E} [\text{softmax}_{y_i} f(\mathbf{x}'_i; \mathbf{w})], \quad (9)$$

$$\mathcal{L}_{\text{logits}}^i(y_i; \mathbf{w}) = \log P_{\text{logits}}(y_i | \mathbf{x}_i, \mathbf{w}) = \log \text{softmax}_{y_i} \mathbb{E} [f(\mathbf{x}'_i; \mathbf{w})]. \quad (10)$$

We can form lower bounds on both these quantities using K -sample estimators,

$$\hat{\mathcal{L}}_{\text{prob}}^i(y_i; \mathbf{w}) = \log \left[\frac{1}{K} \sum_{k=1}^K \text{softmax}_{y_i} f(\mathbf{x}'_{i,k}; \mathbf{w}) \right], \quad (11)$$

$$\hat{\mathcal{L}}_{\text{logits}}^i(y_i; \mathbf{w}) = \log \text{softmax}_{y_i} \left[\frac{1}{K} \sum_{k=1}^K f(\mathbf{x}'_{i,k}; \mathbf{w}) \right]. \quad (12)$$

To prove the lower-bound for averaging probabilities, we take an approach familiar from variational inference (Jordan et al., 1999) by applying Jensen’s inequality to the (concave) logarithm function,

$$\begin{aligned} \mathcal{L}_{\text{prob}}^i(y_i; \mathbf{w}) &= \log \mathbb{E} \left[\frac{1}{K} \sum_{k=1}^K \text{softmax}_{y_i} f(\mathbf{x}'_{i,k}; \mathbf{w}) \right] \\ &\geq \mathbb{E} \left[\log \frac{1}{K} \sum_{k=1}^K \text{softmax}_{y_i} f(\mathbf{x}'_{i,k}; \mathbf{w}) \right] = \mathbb{E} \left[\hat{\mathcal{L}}_{\text{prob}}^i(y_i; \mathbf{w}) \right]. \end{aligned} \quad (13)$$

For averaging logits, we note that $\log \text{softmax}_{y_i}$ is a concave function (Boyd et al., 2004) taking a vector of logits and returning a scalar log-probability for class y_i . As such, we can again apply Jensen’s inequality,

$$\begin{aligned} \mathcal{L}_{\text{logits}}^i(y_i; \mathbf{w}) &= \log \text{softmax}_{y_i} \mathbb{E} \left[\frac{1}{K} \sum_{k=1}^K f(\mathbf{x}'_{i,k}; \mathbf{w}) \right] \\ &\geq \mathbb{E} \left[\log \text{softmax}_{y_i} \frac{1}{K} \sum_{k=1}^K f(\mathbf{x}'_{i,k}; \mathbf{w}) \right] = \mathbb{E} \left[\hat{\mathcal{L}}_{\text{logits}}^i(y_i; \mathbf{w}) \right]. \end{aligned} \quad (14)$$

In practice, we use different numbers of samples at test and training time, K_{test} and K_{train} respectively. Note that Wenzel et al. (2020) gave the single-sample averaging probabilities bound, but did not generalise it to the multi-sample setting.

These bounds have a free parameter, K , raising the question of which values for K are likely to be sensible. Naïvely, we would expect a single-sample estimate of an expectation to have high variance, and high-variance estimators give loose bounds and biased inferences when used with Jensen’s inequality (Liao & Berg, 2018). We do indeed find benefit in using $K_{\text{train}} > 1$ (Fig. 1), single-sample estimates are used frequently in variational inference (VI; Jordan et al., 1999), which suggests they might be viable here too. That said, high variance and hence biased estimators are a problem in VI for the same reason, which is commonly mitigated by using $K > 1$ (Burda et al., 2015; Aitchison, 2018). However, VI incorporates a highly effective variance reduction strategy that is absent in our setting: an optimized variational approximate posterior (see Appendix B). In principle, similar variance reduction strategies exist in our setting, but would involve learning a separate variance-reducing augmentation distribution for each image, which is clearly impractical. In the absence of such a strategy, the only viable approach to reducing variance in the Jensen bound is to use multiple samples, though the exact number of samples required at test and train time is an empirical question.

To support the arguments above that that $K = 1$ is unlikely to be sufficient, note that $K = 1$ represents such a crude approximation that it collapses the differences between averaging probabilities, logits, and losses,

$$\hat{\mathcal{L}}_{\text{logits}}^i(y_i; \mathbf{w}) = \hat{\mathcal{L}}_{\text{prob}}^i(y_i; \mathbf{w}) = \hat{\mathcal{L}}_{\text{loss}}^i(y_i; \mathbf{w}) = \log \text{softmax}_{y_i} f(\mathbf{x}'_{i,k}; \mathbf{w}), \quad (15)$$

while we show empirically that $\hat{\mathcal{L}}_{\text{prob}}$, $\hat{\mathcal{L}}_{\text{logits}}$ and $\hat{\mathcal{L}}_{\text{loss}}$ have significant performance differences when $K > 1$ (Figs. 1 and 2). This collapse is intuitive because no averaging actually occurs if we take $K = 1$. Indeed, the reason that Wenzel et al. (2020) considered only a single-sample estimator of the bound (i.e. $K_{\text{train}} = 1$) is precisely that it is equivalent to the standard data augmentation setup.

Finally, all of the above is for the usual “full orbit” setting, where there is a distribution over a very large, or even infinite number of possible augmentations.¹ However, we can also consider the “finite orbit” setting, where only a very small number of augmentations are available. In the finite orbit

¹We employ the term “orbit” from group theory and function invariance (Kondor, 2008), even though our augmentations do not necessarily form groups. In this work, it refers to the support of $P(\mathbf{x}' | \mathbf{x})$.

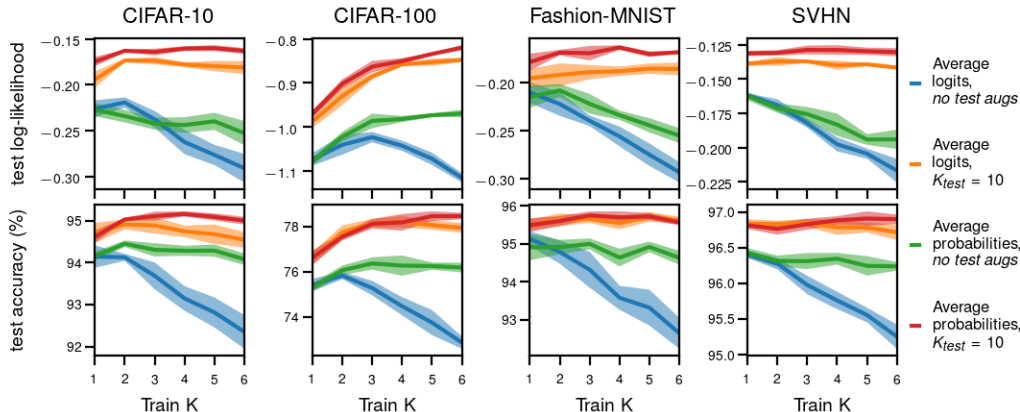


Figure 1: Comparison of averaging logits and probabilities for different values of K_{train} , and using $K_{\text{test}} = 10$ vs. using no test-time augmentations. Here, we use ResNet18 with SGD (i.e. no Bayesian inference). We use only full orbit to decouple K_{train} from K_{test} .

setting, the distribution over augmented images, \mathbf{x}' , conditioned on the underlying unaugmented image, \mathbf{x} , can be written as,

$$P(\mathbf{x}'|\mathbf{x}) = \frac{1}{K} \sum_{k=1}^K \delta(\mathbf{x}' - a_k(\mathbf{x})), \quad (16)$$

where δ is the Dirac-delta, and a_k is a function that applies the k th fixed augmentation. In this setting, it is possible to exactly compute $\mathcal{L}_{\text{logits}}$ and $\mathcal{L}_{\text{prob}}$ by summing over the K augmentations. In practice, we choose the K fixed augmentations by sampling them before training. In the finite orbit setting, we use the same number of augmentations at test and train time, $K_{\text{train}} = K_{\text{test}} = K$.

5 Results

5.1 Principled data augmentation in non-Bayesian networks

We begin by comparing averaging logits and averaging probabilities in a non-Bayesian setting: SGD. Critically, higher values of K_{train} imply more computational cost per epoch, as each image is replicated and augmented K_{train} times before going through the network. To address the question of whether averaging probabilities/logits help in the standard non-Bayesian setting with fixed computational cost, we ensured that almost exactly the same computational budget was used for different methods by training for $200/K_{\text{train}}$ epochs. Note that $K_{\text{train}} = 1$ with no test-time augmentation (i.e. green and blue) corresponds to the standard data augmentation approach for both averaging-logits and averaging-probabilities (Eq. 15). In this experiment, we consider only full orbit, which unlike finite orbit allows us to decouple K_{train} and K_{test} .

We trained ResNet18² on CIFAR10, CIFAR100 (Krizhevsky et al., 2009)³, FashionMNIST (Xiao et al., 2017)⁴ and SVHN (Netzer et al., 2011)⁵ with a learning rate of 0.1, decayed to 0.01 three quarters of the way through training. The training runs took around 12 GPU-days on Nvidia 2080s.⁶

In agreement with past work, we found that averaging over augmentations at test-time (red and orange) is better than using the test image without augmentation (green and blue), with $K_{\text{train}} = 1$, corresponding to the standard data augmentation procedure. In addition, we show that improved performance with multiple test-time augmentations continues to hold for larger values of K_{train} . Thus, if sufficient compute is available at test-time, averaging across augmentations gives an easy method to improve the performance of a pre-trained network.

²<https://github.com/kuangliu/pytorch-cifar>; MIT Licensed

³<https://cs.toronto.edu/~kriz/cifar.html>

⁴<https://github.com/zalandoresearch/fashion-mnist>; MIT Licensed

⁵<http://ufldl.stanford.edu/housenumbers/>

⁶<https://anonymous.4open.science/r/Augmentations-D513/>

Importantly, we see some performance gains with higher values of K_{train} if we focus on the case with test augmentations, though they are somewhat inconsistent across datasets. We see strong improvements for the hardest dataset (CIFAR-100), and smaller improvements that saturate at $K_{\text{train}} = 2$ for CIFAR-10. For Fashion-MNIST and SVHN, the picture is more mixed. We suspect this is because we used a data augmentation strategy tuned for CIFAR-10 and CIFAR-100, rather than these other datasets.

In addition, averaging probabilities seems to give somewhat better performance than averaging logits: compare averaging probabilities vs. logits with test-time augmentation (red vs. orange) and without test-time augmentation (green vs. blue). The performance differences are consistent in both comparisons, though smaller when test-time augmentation is applied.

Indeed, performance falls quite dramatically as K_{train} increases for averaging logits without test-time augmentation (blue). This is an indication that perhaps the underlying neural network actually becomes less invariant as K_{train} increases. This might occur because averaging over multiple augmentations introduces a degree of invariance in and of itself, so there is less need for the underlying neural network to be invariant. We would expect a less-invariant network to have reasonable performance with test-time augmentation (orange) but to give worse performance without test-time augmentation (blue). From a statistical point of view, this is not problematic, as the same likelihood should be applied at test time as at training time, which prescribes augmentation at test time. From a practical point of view however, this behaviour is problematic, as we may want to use a small K_{test} for computational efficiency at test time. In contrast, this does not occur with averaging probabilities: performance is much more constant as K_{train} increases, even when evaluating without test-time augmentation (green).

To understand this difference, we consider the effect of averaging on the NN function itself. Both schemes can be justified by using averaging to increase invariance to the augmentation transformations. Averaging probabilities, however, also forces the NN function itself to become invariant. If different augmentations produce different predictions, then the resulting averaged prediction will be more uncertain, which is penalised by the likelihood on the training points. This effect is much weaker when averaging logits. Consider an extreme example: a two-class classification problem with two augmentations, \mathbf{x}'_1 and \mathbf{x}'_2 , of the same image with logits, $f(\mathbf{x}'_1) = (100, -100)$ and $f(\mathbf{x}'_2) = (-10, 10)$. Averaging logits gives us $\mathbb{E}[f(\mathbf{x}')] = (45, -45)$, and applying the softmax, we very confidently predict the first class. In contrast, if we use averaging probabilities, then the first augmentation almost certainly predicts the first class $p(X'_1) \approx (1, 0)$ and the second augmentation almost certainly predicts the second class, $p(X'_2) \approx (0, 1)$, so when we average them we obtain $\mathbb{E}[p(X')|X] \approx (0.5, 0.5)$, which indicates a high degree of uncertainty.

This provides a potential explanation for the differential effects of increasing K_{train} with no test-time augmentations in Fig. 1. The supervised objective encourages the classifier to be as certain as possible about the true class label. To achieve certainty for averaging probabilities, the predictive distributions for almost all augmentations of the same underlying image need to be concentrated on the true class. This requirement encourages the trained neural network to be invariant to the underlying augmentation, just like in the standard approach to data augmentation. While this happens to some extent with averaging logits, the effect is smaller: as in the above example, it is possible for the overall system to be highly confident about the correct class-label with an underlying network that is less invariant.

5.2 Bayesian neural networks and the cold posterior effect

Next, we ask a very different question: how is the cold posterior effect influenced by using principled data augmentation priors? To this end, we use a different experimental setup. In particular, we take the code⁷ and networks from Fortuin et al. (2021b,a) and mirror their experimental setup as closely as possible. This code combines a cyclical learning rate schedule (Zhang et al., 2019), a gradient-guided Monte Carlo (GG-MC) scheme (Garriga-Alonso & Fortuin, 2021), and the preconditioning and convergence diagnostics from Wenzel et al. (2020). Following Fortuin et al. (2021b), we ran 60 cycles with 45 epochs in each cycle. We recorded one sample at the end of each of the last five epochs of a cycle, giving 300 samples total. Importantly, to allow for running many sampling epochs in these experiments, we follow Fortuin et al. (2021b) in using the ResNet20 architecture from Wenzel et al.

⁷https://github.com/ratschlab/bnn_priors; MIT Licensed

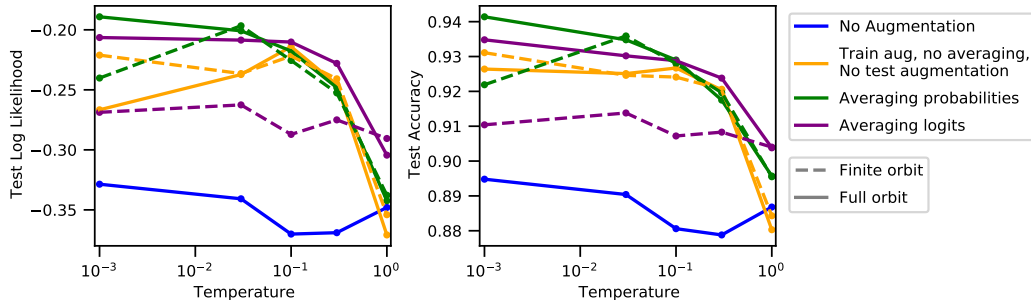


Figure 2: The cold posterior effect for different data augmentation configurations when running GGMC with ResNet20 on CIFAR-10. Without data augmentation, there is a minimal cold posterior effect. Most other configurations show significant improvement for $T < 1$, with the exception of averaging the logits over a fixed orbit. Averages are computed with $K_{\text{train}} = K_{\text{test}} = 8$.

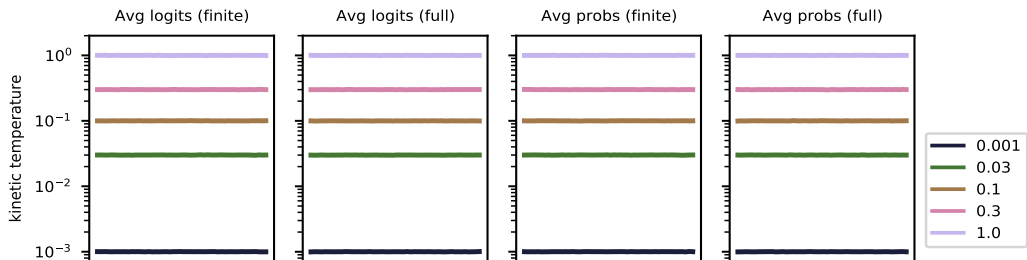


Figure 3: The evolution of the kinetic temperature diagnostic throughout inference. Good agreement between the diagnostic temperature and intended temperature (in legend) suggests accurate inference.

(2020), which is small relative to the ResNet18 used in Sec. 5.1 (i.e. 32 channels for the first block up to 128 in the last block compared to 64 channels up to 512 (He et al., 2016a)). As such, SGD in this network performs poorly compared with that in Sec. 5.1 ($\sim 92\%$ (Wenzel et al., 2020) vs. $\sim 95\%$ (He et al., 2016b)). The experiments took around 60 GPU-days on Nvidia RTX6000s⁸.

The results are presented in Fig. 2. We replicate the finding that the cold posterior effect is largely absent without data augmentation (blue), and is present in the standard setup with data augmentation at training time but without averaging (yellow). Further, we show that the cold posterior effect persists with principled data augmentation priors: averaging logits with full orbit (purple solid line), and averaging probabilities with fixed and full orbits (green). The best method overall appears to be averaging probabilities with a full orbit (solid green line) at a very low temperature, though averaging logits (solid purple line) is better at higher temperatures.

Surprisingly, the cold posterior effect is much smaller for averaging logits with finite orbit (dashed purple line), which demonstrated best performance at $T = 1$ (close to averaged logits over full orbit; solid purple line). However, the relevance of this is unclear, as the reduction in the cold posterior effect arises primarily because of worse low-temperature performance.

The usefulness of these results is contingent on understanding whether we are indeed accurately approximating the posterior. To check, we computed the kinetic temperature, which estimates the temperature of a given parameter in the Langevin dynamics simulation from the norm of its momentum. In expectation, the kinetic temperature estimator should be equal to the desired temperature, T . Fig. 3 shows how all the samplers run at their desired temperature, a result that is consistent with accurate posterior sampling.

⁸anonymous.4open.science/r/bayesian-data-aug/experiments/bayes_data_aug/README.md

6 Related work

Wenzel et al. (2020) introduced the cold posterior effect and considered and rejected many possible explanations. The only hypothesis that they were not able to dismiss was that the model was somehow misspecified. Note that they introduced the averaging probabilities generative model, but considered only $K_{\text{train}} = 1$, for which averaging probabilities, logits and losses become equivalent. As such, they were not able to distinguish the predictions for and differential cold posteriors effects in these three different approaches.

Following up on this work, Fortuin et al. (2021b) explicitly asked whether better priors over the weights would mitigate the cold posterior effect. As averaging logits and averaging probabilities can also be understood as modifying the prior over functions (van der Wilk et al., 2018), this is perhaps the closest prior work. Fortuin et al. (2021b) consider heavy-tailed priors over the weights in small networks and spatially correlated priors over the weights of convolutional filters in large-scale networks. While heavy-tailed priors indeed mitigated the cold posterior effect in small networks, spatially correlated priors improved performance at all temperatures, and thus did not reduce the cold posterior effect. As such, their results are fundamentally in agreement with ours; they, like us, were unable to find priors that mitigated the cold posterior effect in large-scale networks.

Nonetheless, the only possible explanation of the cold posterior effect that Wenzel et al. (2020) were unable to dismiss was that of model misspecification. Our present results, and those of Fortuin et al. (2021b) have not been able to remove the cold posterior effect by changing the prior over neural network functions. So which part is misspecified? Aitchison (2020) suggests that the misspecification can be in the likelihood, not just in the prior over functions. They noted that in heavily curated datasets such as CIFAR-10 and ImageNet, multiple annotators look at each image, and the image is only included in the dataset if they agree. If we take S annotators who all agree about the class-label, the resulting true posterior is

$$P(\mathbf{w}|\mathbf{X}, \mathbf{y}) = P(\mathbf{w}) \prod_{i=1}^N P(y_i|\mathbf{w}, \mathbf{x}_i)^S, \tag{17}$$

where $P(y_i|\mathbf{w}, \mathbf{x}_i)$ is taken to be the single-annotator predictive distribution. Critically, this strongly resembles the cold posterior in Eq. (6) with $S = 1/T$; the main difference being that only the likelihood, and not the prior is modified (see Aitchison, 2020 for further discussion). In this context, the observation that there is no cold posterior effect without augmentation is still puzzling.

One potential resolution is to posit that the right prior must include data augmentation, as evidenced by its undeniable performance benefits. Importantly, while the Bayesian framework states that the true model performs best, it does not say anything about the relative performance of misspecified models. As such, if we think that the “true model” includes both curation and augmentation, then Bayesian theory only predicts that a model with curation and augmentation should perform best. In particular, it does not tell us about the relative performance of misspecified models that lack either curation or data augmentation. In practice, we suspect that the additional certainty provided by data curation only helps generalisation in the context of an invariant model with data augmentation, whereas a non-invariant model without data augmentation may just overfit to the training data.

Contemporaneous work, suggests that in agreement with our results in Fig. 1, using multiple training augmentations improves generalization in large neural networks (Fort et al., 2021). However, they did not work within a principled Bayesian framework as they used averaging losses, and they did not assess any connection to the cold posterior effect. Similarly, Hoffer et al. (2019) and Berman et al. (2019) averaged losses for improving the generalization of models trained with large batches, and Choi et al. (2019) did so for better hardware utilization. Benton et al. (2020) averaged losses in order to learn invariances in neural networks. In this case, there is no difference in the expected training objective for averaging one sample vs. multiple samples, so Benton et al. (2020) used a single sample. Last, the averaging of losses is applied in the context of vision transformers by Touvron et al. (2021).

Averaging probabilities, which we found to perform slightly better than averaging logits, has been used at test time in many image classification works (e.g. Krizhevsky et al., 2012; He et al., 2015; Szegedy et al., 2015; Simonyan & Zisserman, 2014). Averaging logits is less widespread, though “feature averaging”, which is closely related, was used by Foster et al. (2020) to improve test time performance. To our knowledge, neither averaging logits nor probabilities has been used at training time.

Past work purely in the Gaussian process (GP) context introduced a principled generative model incorporating averaging logits (van der Wilk et al., 2018). However, they did not apply the method to (convolutional) neural networks, e.g. in modern image classification settings and they did not consider either averaging probabilities or the cold posterior effect.

A considerable body of past work on Bayesian inference in neural networks, using both variational inference (Blundell et al., 2015) and stochastic gradient Langevin dynamics (Welling & Teh, 2011) uses data augmentation (e.g. Zhang et al., 2018, 2019; Osawa et al., 2019; Fortuin et al., 2021b; Immer et al., 2021). However, as discussed in Sec. 3 (Background), these methods simply substitute non-augmented for augmented data and thus do not use a valid log-likelihood. In contrast, we incorporated data augmentation into the probabilistic generative model, and thus are able to give valid log-likelihoods based on averaging logits or averaging probabilities.

7 Conclusions

We considered two principled probabilistic generative models incorporating data augmentation. We found that they give improved performance in standard SGD settings with a fixed compute budget. In addition, we looked at their interaction with the cold posterior effect. The cold posterior effect did not go away when using principled data augmentation, suggesting that the question of dataset size in data augmentation may not provide an explanation of the cold posterior effect. Instead, these results are consistent with an alternative theory of the cold posterior effect, which introduces a probabilistic generative model describing data curation (Aitchison, 2020). No particular negative social impacts are anticipated as this is largely theoretical work.

References

- Aitchison, L. Tensor Monte Carlo: particle methods for the GPU era. *arXiv preprint arXiv:1806.08593*, 2018.
- Aitchison, L. A statistical theory of cold posteriors in deep neural networks. *arXiv preprint arXiv:2008.05912*, 2020.
- Benton, G., Finzi, M., Izmailov, P., and Wilson, A. G. Learning invariances in neural networks. *arXiv preprint arXiv:2010.11882*, 2020.
- Berman, M., Jégou, H., Vedaldi, A., Kokkinos, I., and Douze, M. Multigrain: a unified image embedding for classes and instances. *arXiv preprint arXiv:1902.05509*, 2019.
- Bishop, C. M. *Pattern recognition and machine learning*. springer, 2006.
- Blundell, C., Cornebise, J., Kavukcuoglu, K., and Wierstra, D. Weight uncertainty in neural network. In *International Conference on Machine Learning*, pp. 1613–1622. PMLR, 2015.
- Boyd, S., Boyd, S. P., and Vandenberghe, L. *Convex optimization*. Cambridge university press, 2004.
- Burda, Y., Grosse, R., and Salakhutdinov, R. Importance weighted autoencoders. *arXiv preprint arXiv:1509.00519*, 2015.
- Chen, S., Dobriban, E., and Lee, J. H. A group-theoretic framework for data augmentation. *Journal of Machine Learning Research*, 21(245):1–71, 2020. URL <http://jmlr.org/papers/v21/20-163.html>.
- Choi, D., Passos, A., Shallue, C. J., and Dahl, G. E. Faster neural network training with data echoing. *arXiv preprint arXiv:1907.05550*, 2019.
- Dao, T., Gu, A., Ratner, A., Smith, V., De Sa, C., and Re, C. A kernel theory of modern data augmentation. In Chaudhuri, K. and Salakhutdinov, R. (eds.), *Proceedings of the 36th International Conference on Machine Learning*, volume 97 of *Proceedings of Machine Learning Research*, pp. 1528–1537. PMLR, 09–15 Jun 2019. URL <http://proceedings.mlr.press/v97/dao19b.html>.

- Fort, S., Brock, A., Pascanu, R., De, S., and Smith, S. L. Drawing multiple augmentation samples per image during training efficiently decreases test error. *arXiv preprint arXiv:2105.13343*, 2021.
- Fortuin, V. Priors in bayesian deep learning: A review. *arXiv preprint arXiv:2105.06868*, 2021.
- Fortuin, V., Garriga-Alonso, A., van der Wilk, M., and Aitchison, L. BNNpriors: A library for Bayesian neural network inference with different prior distributions. *Software Impacts*, pp. 100079, 2021a.
- Fortuin, V., Garriga-Alonso, A., Wenzel, F., Rätsch, G., Turner, R., van der Wilk, M., and Aitchison, L. Bayesian neural network priors revisited. *arXiv preprint arXiv:2102.06571*, 2021b.
- Foster, A., Pukdee, R., and Rainforth, T. Improving transformation invariance in contrastive representation learning. *arXiv preprint arXiv:2010.09515*, 2020.
- Garriga-Alonso, A. and Fortuin, V. Exact Langevin dynamics with stochastic gradients. *arXiv preprint arXiv:2102.01691*, 2021.
- He, K., Zhang, X., Ren, S., and Sun, J. Delving deep into rectifiers: Surpassing human-level performance on ImageNet classification. In *Proceedings of the IEEE international conference on computer vision*, pp. 1026–1034, 2015.
- He, K., Zhang, X., Ren, S., and Sun, J. Deep residual learning for image recognition. In *Proceedings of the IEEE conference on computer vision and pattern recognition*, pp. 770–778, 2016a.
- He, K., Zhang, X., Ren, S., and Sun, J. Identity mappings in deep residual networks. In *European conference on computer vision*, pp. 630–645. Springer, 2016b.
- Hoffer, E., Ben-Nun, T., Hubara, I., Giladi, N., Hoefler, T., and Soudry, D. Augment your batch: better training with larger batches. *arXiv preprint arXiv:1901.09335*, 2019.
- Immer, A., Bauer, M., Fortuin, V., Rätsch, G., and Khan, M. E. Scalable marginal likelihood estimation for model selection in deep learning. *arXiv preprint arXiv:2104.04975*, 2021.
- Izmailov, P., Vikram, S., Hoffman, M. D., and Wilson, A. G. What are Bayesian neural network posteriors really like? *arXiv:2104.14421*, 2021.
- Jordan, M. I., Ghahramani, Z., Jaakkola, T. S., and Saul, L. K. An introduction to variational methods for graphical models. *Machine learning*, 37(2):183–233, 1999.
- Kondor, I. R. *Group theoretical methods in machine learning*. 2008.
- Krizhevsky, A., Hinton, G., et al. Learning multiple layers of features from tiny images. 2009.
- Krizhevsky, A., Sutskever, I., and Hinton, G. E. ImageNet classification with deep convolutional neural networks. *Advances in neural information processing systems*, 25:1097–1105, 2012.
- Liao, J. and Berg, A. Sharpening Jensen’s inequality. *The American Statistician*, 2018.
- Loog, M., Viering, T., and Mey, A. Minimizers of the empirical risk and risk monotonicity. *arXiv preprint arXiv:1907.05476*, 2019.
- Loosli, G., Canu, S., and Bottou, L. Training invariant support vector machines using selective sampling. *Large scale kernel machines*, 2, 2007.
- MacKay, D. J. A practical Bayesian framework for backpropagation networks. *Neural computation*, 4(3):448–472, 1992.
- Netzer, Y., Wang, T., Coates, A., Bissacco, A., Wu, B., and Ng, A. Y. Reading digits in natural images with unsupervised feature learning. *NIPS Workshop on Deep Learning and Unsupervised Feature Learning 2011*, 2011.
- Osawa, K., Swaroop, S., Jain, A., Eschenhagen, R., Turner, R. E., Yokota, R., and Khan, M. E. Practical deep learning with Bayesian principles. *arXiv preprint arXiv:1906.02506*, 2019.

- Shorten, C. and Khoshgoftaar, T. M. A survey on image data augmentation for deep learning. *Journal of Big Data*, 6(1):1–48, 2019.
- Simonyan, K. and Zisserman, A. Very deep convolutional networks for large-scale image recognition. *arXiv preprint arXiv:1409.1556*, 2014.
- Szegedy, C., Liu, W., Jia, Y., Sermanet, P., Reed, S., Anguelov, D., Erhan, D., Vanhoucke, V., and Rabinovich, A. Going deeper with convolutions. In *Proceedings of the IEEE conference on computer vision and pattern recognition*, pp. 1–9, 2015.
- Touvron, H., Cord, M., Sablayrolles, A., Synnaeve, G., and Jégou, H. Going deeper with image transformers. *arXiv preprint arXiv:2103.17239*, 2021.
- van der Wilk, M., Bauer, M., John, S., and Hensman, J. Learning invariances using the marginal likelihood. *arXiv preprint arXiv:1808.05563*, 2018.
- Welling, M. and Teh, Y. W. Bayesian learning via stochastic gradient Langevin dynamics. In *Proceedings of the 28th international conference on machine learning (ICML-11)*, pp. 681–688. Citeseer, 2011.
- Wenzel, F., Roth, K., Veeling, B. S., Świątkowski, J., Tran, L., Mandt, S., Snoek, J., Salimans, T., Jenatton, R., and Nowozin, S. How good is the Bayes posterior in deep neural networks really? *arXiv preprint arXiv:2002.02405*, 2020.
- Xiao, H., Rasul, K., and Vollgraf, R. Fashion-MNIST: a novel image dataset for benchmarking machine learning algorithms. *arXiv preprint arXiv:1708.07747*, 2017.
- Zhang, G., Sun, S., Duvenaud, D., and Grosse, R. Noisy natural gradient as variational inference. In *International Conference on Machine Learning*, pp. 5852–5861. PMLR, 2018.
- Zhang, R., Li, C., Zhang, J., Chen, C., and Wilson, A. G. Cyclical stochastic gradient MCMC for Bayesian deep learning. *arXiv preprint arXiv:1902.03932*, 2019.

A Averaging losses emerges when using data augmentation in VI and SGLD

There are two particularly important algorithms for doing Bayesian inference in neural networks: stochastic gradient Langevin dynamics (SGLD; Welling & Teh, 2011) and variational inference (VI; Blundell et al., 2015). In SGLD without data augmentation, we draw samples from the posterior over weights by following gradient of the log-probability with added noise,

$$(\Delta \mathbf{w})_{\text{noaug}} = \frac{\epsilon}{2} \nabla_{\mathbf{w}} \left[\log P(\mathbf{w}) + \sum_{i=1}^N \log P_{\text{noaug}}(y_i | \mathbf{x}_i, \mathbf{w}) \right] + \sqrt{\epsilon} \boldsymbol{\eta} \quad (18)$$

where $\boldsymbol{\eta}$ is standard Gaussian IID noise, and for simplicity we give the expression for full-batch Langevin dynamics rather than minibatched SGLD (they do not differ for the purposes of reasoning about data augmentation). Likewise the variational inference objective is,

$$\text{ELBO}_{\text{noaug}} = \mathbb{E}_{Q(\mathbf{w})} \left[\log P(\mathbf{w}) + \sum_{i=1}^N \log P_{\text{noaug}}(y_i | \mathbf{x}_i, \mathbf{w}) - \log Q(\mathbf{w}) \right] \quad (19)$$

where $Q(\mathbf{w})$ is the variational approximate posterior learned by optimizing this objective. To understand the overall effect of this approach to data augmentation, we replace $\log P_{\text{noaug}}(y_i | \mathbf{x}_i, \mathbf{w})$ with the log-softmax using Eq. (2). Then, we consider the expected update to the weights, averaging over the augmented images, \mathbf{x}'_i conditioned on the underlying unaugmented images, \mathbf{x}_i ,

$$\mathbb{E} \left[(\Delta \mathbf{w})_{\text{aug}} \right] = \frac{\epsilon}{2} \nabla_{\mathbf{w}} \left[\log P(\mathbf{w}) + \sum_{i=1}^N \mathcal{L}_{\text{loss}}^i(y_i; \mathbf{w}) \right] + \sqrt{\epsilon} \boldsymbol{\eta}, \quad (20)$$

$$\text{ELBO}_{\text{aug}} = \mathbb{E}_{Q(\mathbf{w})} \left[\log P(\mathbf{w}) + \sum_{i=1}^N \mathcal{L}_{\text{loss}}^i(y_i; \mathbf{w}) - \log Q(\mathbf{w}) \right]. \quad (21)$$

In both cases, this ultimately replaces $\log P_{\text{noaug}}(y_i | \mathbf{x}_i, \mathbf{w})$ with $\mathcal{L}_{\text{loss}}^i(y_i; \mathbf{w})$, which as discussed in Sec. 3.1 is not a valid log-likelihood.

B The approximate posterior in VI reduces variance

Here, we derive the ELBO using Jensen’s inequality; we take x to be the data and z to be a latent variable. Our goal is to compute the model evidence, $P(x)$, by integrating out z ,

$$P(x) = \int dz P(x|z) P(z) = \int dz P(x, z) \quad (22)$$

where $P(z)$ is the prior, $P(x|z)$ is the likelihood and $P(x, z)$ is the joint. We introduce an approximate posterior, $Q(z)$, and rewrite the integral as an expectation over that approximate posterior and apply Jensen’s inequality,

$$\log P(x) = \log \int dz Q(z) \frac{P(x, z)}{Q(z)} \quad (23)$$

$$= \log \mathbb{E}_{Q(z)} \left[\frac{P(x, z)}{Q(z)} \right] \geq \mathbb{E}_{Q(z)} \left[\log \frac{P(x, z)}{Q(z)} \right]. \quad (24)$$

Now it is evident that the tightness of the bound is controlled by the variance of $P(x, z) / Q(z)$. Critically, if $Q(z)$ matches the true posterior,

$$Q(z) = P(z|x) \propto P(x, z) \quad (25)$$

then $P(x, z) / Q(z)$ is constant (zero variance) and the bound is tight.